Physics of the Earth and Planetary Interiors xxx (2008) xxx–xxx

Contents lists available at ScienceDirect

Physics of the Earth and Planetary Interiors

journal homepage: www.elsevier.com/locate/pepi

New measurements of activation volume in olivine under anhydrous conditions

W.B. Durham[a,*], S. Mei[b], D.L. Kohlstedt[b], L. Wang[c], N.A. Dixon[a]

[a] Massachusetts Institute of Technology, Cambridge, MA 02139, United States
[b] University of Minnesota, Minneapolis, MN 55455, United States
[c] Stony Brook University, Stony Brook, NY 11794, United States

ARTICLE INFO

Article history:
Received 16 November 2007
Received in revised form 18 July 2008
Accepted 28 July 2008

Keywords:
Olivine deformation
Activation volume
Dry olivine
Rheology of olivine
D-DIA

ABSTRACT

A new cell assembly for the deformation-DIA (D-DIA) shows promise for limiting the water content of samples and providing a more mechanically stable environment for deformation. The 6-mm cubic cell consists of a 6-mm diameter mullite sphere cradled in a web of unfired pyrophyllite. The pyrophyllite flows during initial compression of the D-DIA to form gaskets between the six anvils while the mullite flows to become a nearly cubic-shaped pressure medium. Measurements on olivine indicate more than one order of magnitude drop in water content to <40 ppm H/Si compared with the boron-epoxy medium. Improved mechanical stability is achieved by elimination of the thermocouple from the assembly and determination of temperature from calibration curves of furnace power vs. temperature. Three samples of polycrystalline orthopyroxene-buffer San Carlos olivine have been deformed in high-temperature creep in the new cell, at pressures of 2.7–4.9 GPa and temperatures near 1473 K. Strength is consistent with that measured in the gas-apparatus at lower pressures. Over the pressure range investigated we resolve an activation volume for creep of dry olivine of $V^* = 9.5 \pm 7 \times 10^{-6}$ m^3/mol.

1. Introduction

Critical parameters in geodynamics are many, but few are as elusive as the activation volume for creep of olivine. It can be expected that the properties of olivine control much of Earth's character because it is the major phase of the upper mantle, which transcends a pressure range from approximately 0.3 to 15 GPa to a depth of 400 km. In particular, the rheological properties of olivine are key to the thermal structure and dynamic behavior of the upper mantle. Measurement of the pressure dependence of the viscosity of olivine has been a goal of experimentalists almost since the earliest test of olivine-bearing rock under pressure nearly a half-century ago (Griggs et al., 1960).

Activation volume, V^*, which measures the response of high-temperature, steady-state deformation of a rock to hydrostatic pressure, P, is given by:

$$\dot{\varepsilon} \propto \exp\left(\frac{E^* - PV^*}{RT}\right) \quad (1)$$

where $\dot{\varepsilon}$ is creep rate, T is temperature, and R is the gas constant. The greatest barrier to a well-resolved measurement of V^* has been a limit on achievable pressures in the laboratory, which, until the recent advent of a new generation of high-pressure deformation apparatus, was about 2 GPa using the solid-medium Griggs apparatus. We report here first results from the deformation-DIA, which raises this limit by over a factor of two.

The gas apparatus, with a pressure limit of ~0.5 GPa, has provided well-resolved dependences of creep response on a spectrum of rheologically relevant variables, but rarely of pressure. Recent experiments with a gas apparatus, however, have succeeded in determining a value of $V^* = 23 \times 10^{-6}$ m^3/mol (Wang, 2002). Measurements in the solid-medium Griggs apparatus have extended the pressure to ~2 GPa. Ross et al. (1979) measured $V^* \approx 13 \times 10^6$ m^3/mol using a Griggs apparatus with an external force gage. Stress resolution in such machines is limited because the pressure medium itself has a finite strength, friction on the moving piston is large, and an internal load cell is not easily accommodated in the apparatus. Borch and Green (1989), who solved the problem of strength of the medium by using a molten salt cell within the Griggs rig, measured $V^* = 28 \times 10^6$ m^3/mol, although their samples may have had a high water content (Hirth and Kohlstedt, 1996). More recently Karato and Jung (2003) using the Griggs rig in combination with high-resolution measurements of dislocation density to determine stress, reported values of 14×10^6 m^3/mol under dry conditions and 24×10^6 m^3/mol (after correction) under water-saturated conditions.

Estimates of V^* for high-temperature creep through measurement of more experimentally approachable proxies have been

* Corresponding author.
E-mail address: wbdurham@mit.edu (W.B. Durham).

0031-9201/$ – see front matter © 2008 Elsevier B.V. All rights reserved.
doi:10.1016/j.pepi.2008.07.045

sought, again producing a wide range of results. For dislocation recovery, a necessary step in dislocation creep, Kohlstedt et al. (1980) measured $V^* = 19 \times 10^{-6}$ m^3/mol between 0 and 0.5 GPa; in similar experiments in a solid-medium multi-anvil apparatus Karato et al. (1993) measured $V^* = 6 \times 10^{-6}$ m^3/mol between 0 and 10 GPa. Lattice self-diffusion is a creep mechanism in and of itself and may play a role in dislocation creep as well. The pressure dependence of the diffusion of Si, the slowest diffusing species in olivine, and a subject to which Olivier Jaoul devoted an important part of his career, is $V^* \approx 0$ m^3/mol under pressures to 9 GPa (Bejina et al., 1997, 1999; Jaoul, 1990). Recent diffusion experiments suggest that V^* for Si self-diffusion is actually somewhat >0 m^3/mol (Dohmen et al., 2002). Borch and Green (1987, 1989), who argue that the pressure dependence for creep and for the solidus temperature are closely related, suggest a V^* for creep in olivine close to 30×10^{-6} m^3/mol. The validity of these estimates depends of course on the relationship of the various proxies to creep deformation; they may be more or less related depending on deformation mechanism.

Activation energy is probably pressure dependent, in part because elastic moduli are pressure dependent (Poirier and Liebermann, 1984). Additionally Raterron et al. (this volume) have found a variation in pressure dependence of slip in single crystals of olivine depending on slip system. Since the slip system that controls the dislocation creep rate can change with conditions that themselves are pressure dependent, such as water content, pressure dependence of flow in the mantle may be quite complex.

With a range of possible values for $V^*$of 6 to 30×10^{-6} m^3/mol, the range of allowable viscosities for olivine at the base of the upper mantle is nearly 10 orders of magnitude. Even considering that some of the observed variation in V^* is explicable by water weakening of olivine and the effect of pressure on water content (Hirth and Kohlstedt, 2003) and by the effect of pressure on creep mechanism (Hirth and Kohlstedt, 2003; Raterron et al., this volume), the rheological behavior of the lower part of the upper mantle is, at best, very poorly constrained.

Although not the only motivation, the quest for V^* in olivine provided researchers with strong incentive to develop the next generation of high-pressure deformation machines, made possible by the availability about three decades ago of bright and stable synchrotron × radiation. Non-steady state deformation experiments were possible in quasi-hydrostatic multi-anvil devices and in diamond-anvil cells to $P >$ or $\gg 10$ GPa, respectively (e.g., Durham et al. (2002)). Several years ago two complementary pieces of creep-specialized, synchrotron-ready, high-pressure apparatus were simultaneously developed, the deformation-DIA (D-DIA) (Wang et al., 2003) and rotational Drickamer apparatus (RDA) (Yamazaki and Karato, 2001). The D-DIA, with a design limit of $P \approx$ GPa, was used in the experiments presented in this paper as it is somewhat better suited to measuring simple parameters in the standard flow law.

Over 5 years have passed since the first successful operation of the D-DIA. Measurements of V^* are only now beginning to emerge. One of the main limitations is related to obtaining an anhydrous environment around the sample due to the use of water-bearing pressure media (Li et al., 2006). Another has been a persistently fragile deformation column. We believe that we now have a solution for the last two problems, making it possible to finally report a robust value for V^*.

2. Experiments

The deformation experiments were conducted in a D-DIA apparatus (Wang et al., 2003) installed at beam line X17B2, National Synchrotron Light Source, Brookhaven National Lab. Synchrotron radiation provides the means of determining the state of stress within the sample: X-ray diffraction leads through Bragg's law to the value of lattice spacing as a function of angle to applied load, and hence to the state of elastic strain. The latter is then converted to stress using Hooke's law and the known elastic constants of the material, based on the elastic analysis developed by Singh (1993) and Singh et al. (1998). The method is succinctly summarized in Merkel (2006). Direct X radiography provides images of the sample as a function of time, from which plastic strain rate can be calculated.

The state of stress in a sample under load in the D-DIA is axisymmetric, with the maximum load applied vertically. The X-ray beam enters the cell horizontally. For these experiments we used white X-ray illumination, and detected diffraction in energy dispersive mode. We ran the D-DIA with just one X-ray transparent (polycrystalline diamond) anvil, which allowed detection of diffraction at 0°, 90°, and 180° azimuth around the direct X-ray beam, 0° being vertical, providing sufficient information to determine maximum, minimum, and mean stress. Opaque tungsten carbide anvils at the other three horizontal locations allowed imaging of sample length during deformation. Imaging of the full form of the sample was only possible following depressurization by removing all 4 horizontal anvils, from which we could qualitatively judge the uniformity of the deformation.

A sketch of a typical 6-mm sample deformation cell used in the D-DIA is shown in Fig. 1. The cell fills the cubic void defined by the truncated tips of the six anvils, and comprises the pressure gaskets and pressure medium (which together account for most of the volume of the cell), the furnace, sometimes a thermocouple, and the deformation column. The cylindrical deformation column consists of the sample and two hard alumina pistons, one above and the other below the sample, which itself is wrapped in Ni foil. The D-DIA cell is self-gasketing, in that the gaskets between the six anvils are extruded from cell material as inward displacement (i.e., pressure) is applied by the anvils to the cell. Fabricated gaskets have been successfully included in the assembly for the DIA, but are rarely used as they involve a large number of very small parts (Wang, personal communication).

The polycrystalline olivine studied here is cored from a charge of powdered San Carlos olivine + 5% by mass enstatite (to fix the activity of Si) that is hot pressed for 4 h in a Ni capsule at 1473 K at 300 MPa gas pressure. The starting material has an olivine grain size of ~6 μm and a resultant hot-pressed sample has porosity of <1%. To minimize water content in the sample and its assembly, all parts are vacuum baked at 423 K for >10 h before assembly. For 12–24 h prior to testing, the finished assembly (the "cell") is stored under vacuum at $T >$ 373 K.

We follow a normal experimental protocol for measuring rheological properties: the cell is pressurized hydrostatically at room temperature while suppressing sample shape change (Fig. 1), power is then applied to the graphite heater to bring the sample to run temperature, and finally compressional displacement of the differential rams of the D-DIA is initiated and continued at a fixed rate until the desired strain is reached. The length is typically shortened by 10–15% in our steps, which is usually sufficient to pass through major transients and into a quasi steady-state deformation regime. The compressional step lasts for 1 h up to many hours depending on displacement rate, during which time we record sample length and diffraction spectra. During deformation we slowly drain hydraulic fluid from the main press in order to maintain pressure (i.e., mean stress) at a constant level. The rate at which we relieve the force of the main press is currently based on accumulated experience. We intend in the near future to develop the means for instant analysis of diffraction spectra to allow real-time monitoring (and maintenance of constant pressure).

Please cite this article in press as: Durham, W.B., et al., New measurements of activation volume in olivine under anhydrous conditions. Phys. Earth Planet. Interiors (2008), doi:10.1016/j.pepi.2008.07.045

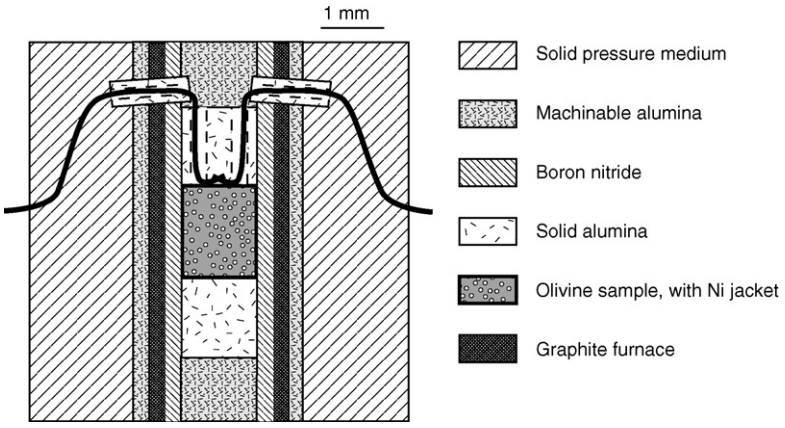

Fig. 1. Scaled section of the cubic sample assembly used for deformation experiments in the D-DIA. The thermocouple (depicted in black) may be removed, in which case the column within the boron nitride sleeve becomes symmetric with respect to the center plane of the sample. The machinable alumina at the ends of this deformation column serves to absorb the approximately 1 mm shortening imposed on the cell during pressurization, limiting any premature deformation of the sample. Active advancing or withdrawal of the differential pistons of the D-DIA is also sometimes used to accomplish the same thing. Section is shown parallel to the cube face; note that thermocouple wires actually emerge at cube edges.

We analyze our results in terms of a power law equation of the form:

$$\dot{\varepsilon}(\sigma, T, P) = A\sigma^n \exp\left(-\frac{E^* + PV^*}{RT}\right) \quad (2)$$

where $\dot{\varepsilon}$ is axial strain rate, as calculated from x radiographs; σ is differential stress, calculated from the diffraction patterns as described above. Our objective is to identify the four material parameters: A, the pre-exponential; n, the stress exponent; E^*, the activation energy; V.

The advance reported here has come about through two recent changes to the cell, both aimed at correcting earlier attempts to measure rheological behavior of olivine using the D-DIA: (1) a choice of cell materials that maintains anhydrous conditions around the sample, and (2) elimination of the thermocouple from the assembly. The key to the anhydrous assembly is a self-gasketing D-DIA cube of hybrid composition: a sphere of mullite embedded in a cube of unfired pyrophyllite, where the diameter of the sphere matches the edge length of the cube (Fig. 2). Unfired pyrophyllite is an excellent gasketing material, being soft and (in notable contrast with mullite) non-friable. Additionally, as a cube-filling "web" around the mullite sphere, the pyrophyllite is ideally configured for D-DIA gasketing (Fig. 2b): maximum volume at the cube corners, minimum (zero) volume at the center of cube faces. Thus the configuration under pressure is a bone-dry mullite pressure medium gasketed by pyrophyllite. Fourier-transform infrared (FTIR) spectroscopy of single crystals hot pressed in the D-DIA in the hybrid cell confirms a low 35–40 H/10^6 Si water content of the olivine, as illustrated in Fig. 3.

Elimination of the thermocouple from the cell assembly results in a demonstrably more symmetric and mechanically stable environment in and around the deformation column throughout an experiment (Fig. 4). Note in Fig. 1 that the volume dedicated to thermocouple wires and to void space around the wires and at the thermocouple tip is a substantial fraction of that of the whole deformation column (pistons + sample), such that the slightly irregular shape of the thermocouple too often leads to complex tractions at the end of the sample, non-parallelism of the ends of the sample, and even catastrophic buckling or transverse slippage of column parts. Earlier studies of deformation in hydrostatic multi-anvil devices (Durham and Rubie, 1998) have demonstrated excellent reproducibility of temperature vs. power vs. time when cell assembly configurations and dimensions are carefully reproduced, which leads us to hypothesize that the absence of a thermocouple in the present assembly can be reliably compensated by off-line calibrations using a thermocouple.

Our strategy in calibrating temperature is to use identical equipment and reproduce all run conditions except sample material: pressure, temperature, D-DIA ram displacement rate, and run time. In a stepping experiment, in which conditions are changed at least once during the run, the calibration must faithfully reproduce the order of steps. (We assume that the presence of X-rays is not nec-

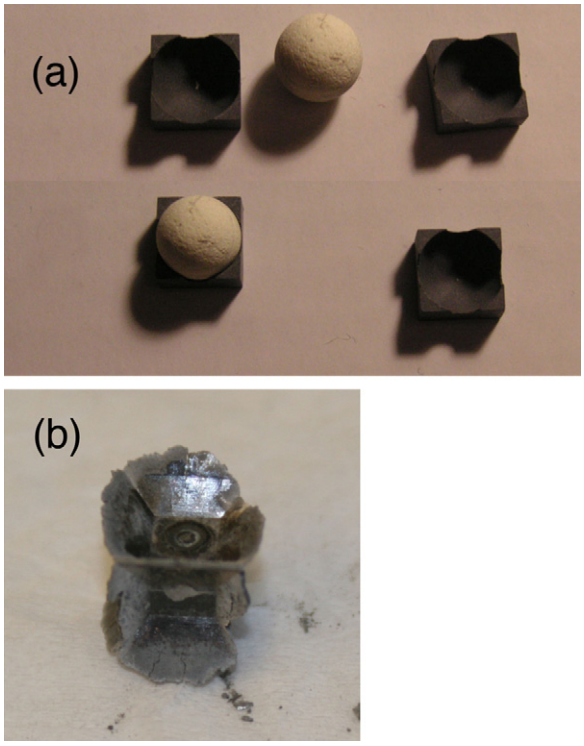

Fig. 2. The new hybrid cell. (a) Cube parts. A 6-mm diameter mullite sphere is cradled and lightly cemented between two pieces of unfired pyrophyllite to form a solid cube of 6-mm edge length. Coring of the hole for furnace and deformation column (Fig. 1) then follows. (b) Appearance of cell following testing in the D-DIA. Gasketing "fins" (some are broken off) of pyrophyllite have been extruded at the edges the cubic cell, now approximately 5 mm in edge length. A spot of mullite is visible on the front face, but no mullite has extruded into the gaskets. The top of the deformation column is visible at the center of the top face.

Please cite this article in press as: Durham, W.B., et al., New measurements of activation volume in olivine under anhydrous conditions. Phys. Earth Planet. Interiors (2008), doi:10.1016/j.pepi.2008.07.045

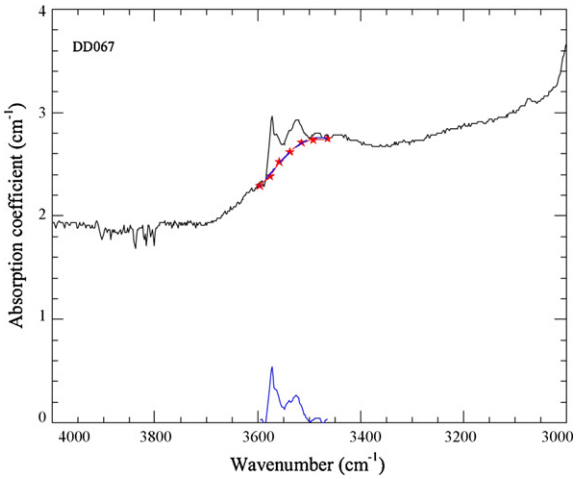

Fig. 3. FTIR spectrum from an olivine single crystal annealed in the hybrid cell for 10 h at 1473 K and a pressure of approximately 6 GPa. The single crystal was of roughly the same size and shape as our polycrystalline deformation samples. The broad background results from contamination introduced by epoxy used to mount the sample. Integration of the IR absorption peaks between 3450 and 3600 cm^{-1}, which are OH stretching bands, yields a hydroxyl content of ~40 ppm H/Si based on the calibration of Paterson (1982). Diffusion measurements reported by Kohlstedt and Mackwell (1998) indicate that after 10 h at 1473 K hydrogen will be incorporated in an olivine crystal up to a depth of 2 mm, assuring that our fine-grained polycrystalline sample was well-equilibrated with the water in its surroundings.

essary, thus conserving valuable beam time by running calibration tests when the X-ray beam is not available.) Furthermore, we can place the calibration thermocouple in the center of the sample, which impossible in a deformation experiment. Our first calibration tests, carried out as a part of the present study, have supported the calibration hypothesis. An example of the good reproducibility in duplicate assemblies of furnace power vs. temperature over short time periods is shown in Fig. 5. The effect of time and deformation (not illustrated) is substantial. As an example, over the course of 12 h and 20% strain at fixed power temperature will increase several tens of Kelvins.

The temperatures of the three runs in this study were estimated on the basis of two calibration runs whose conditions and steps were similar, but not identical, to those of actual tests. The calibration is therefore not as accurate as it will be as we continue to add thermocouple runs to the calibration dataset. For this reason, absolute temperature uncertainty in this study is quite high, although because cells are identical and the temperature range covered is only 100 K, the relative temperature uncertainty between runs is low. A quantitative discussion of error follows below.

3. Results and analysis

To date we have carried out three experiments using the hybrid assembly, at a narrow range of temperatures near 1473 K, strain rates of 2×10^{-6} to 2×10^{-5} s^{-1}, and pressures of 2.7–4.9 GPa. This latter pressure limit was a self-imposed strategy for conserving expensive X-ray transparent polycrystalline diamond (PCD) anvils. While we continue researching materials technology that will allow us X-ray transparency at the known 15 GPa limit of the D-DIA tooling, we felt that the marginal ~1 GPa gain in taking current PCD anvils to their expected breaking point did not justify the high cost of replacing anvils every run, especially given the fact that we had already more than doubled the current experimental limit on pressure in high-temperature creep experiments.

Strain rate and pressure were stepped individually in two of the experiments, giving 5 sets of ($\dot{\varepsilon}$, σ, P, T). The entirety of the

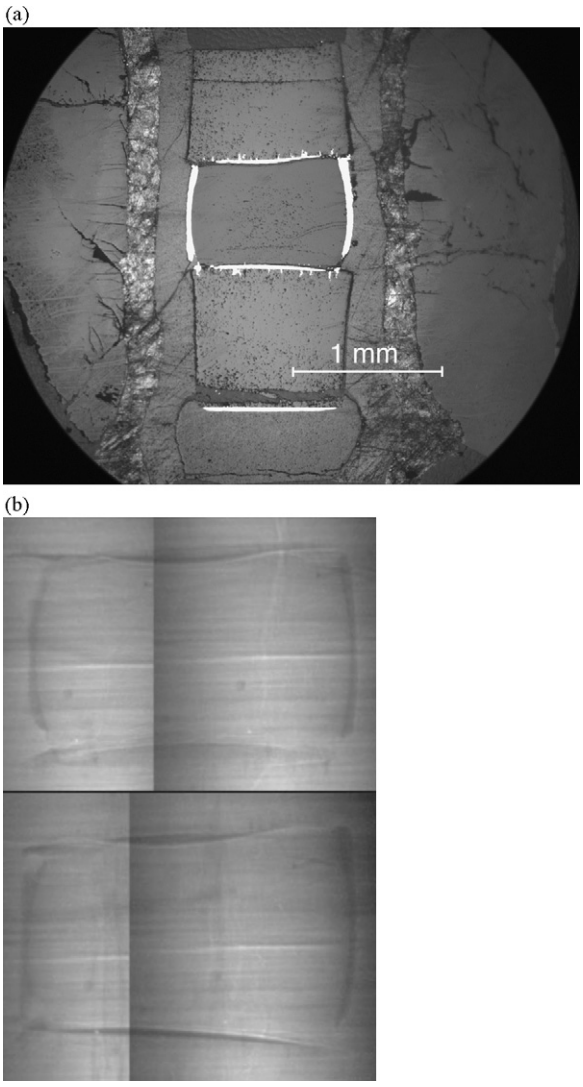

Fig. 4. (a) Optical reflected-light section sample san144 showing good structure of the column The olivine sample sits in the center, surrounded by (bright) Ni foil. (b) X radiographs of san144 viewed in orthogonal directions. The outline of the sample is defined by the Ni foil surrounding the sides and top (the olivine itself is nearly transparent). The sample has shortened by about 30% but still remains approximately a right cylinder, suggesting good uniformity of deformation in the olivine.

creep data are plotted in Fig. 6. Table 1 gives the run conditions and summarizes the results from Fig. 6. Table 1 includes several values differential stress for each run, one for each of three ($h\,k\,l$) reflections as explained in the paragraph to follow, and a fourth "bulk" stress representing an approximate mean of the three. The differential stress values apply to the "apparent" steady state portion of the creep curves where stresses tend to flatten out. There is considerable uncertainty in these estimates, as discussed below.

The improved mechanical performance of the cell was dramatic. The creep curves in Fig. 6 take a generally classic form of a material that reaches a steady state after a shortening of a few percent (e.g., Poirier, 1985, Chpt. 1). The improved mechanical stability of the deformation column is further evident in the good form at the end of the experiment of the deformation column and of the Ni canister around the sample (Fig. 4). The Ni foil at the ends of the sample remained nearly flat and parallel (making shortening measurements easy), and the frequent small gasket slippages ("mini-blowouts") that plagued our efforts with a cell of mullite

Please cite this article in press as: Durham, W.B., et al., New measurements of activation volume in olivine under anhydrous conditions. Phys. Earth Planet. Interiors (2008), doi:10.1016/j.pepi.2008.07.045

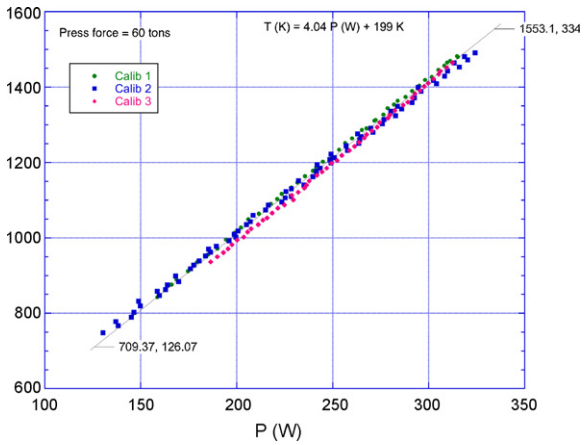

Fig. 5. Off-line calibration of central temperature in the hybrid cell vs. furnace power under 60 T load (corresponding to ~5 GPa at 1500 K). The calibration cell is identical to that shown in Fig. 1, but with the sample removed and the alumina pistons extended such that the thermocouple tip is at the center of the cell. The three calibrations were conducted over a 3-month interval.

only are absent. The performance with earlier cell designs was so poor that we found great reassurance in qualitative observations during the present runs of what one might otherwise take for granted: a strong positive effect of pressure (Fig. 6b) and strain rate (Fig. 6c) and a clear stress relaxation response in step 145(2) (Fig. 6c) when the differential rams were inadvertently halted for 12 min.

Measurement uncertainty (Table 1) is significant and still somewhat difficult to estimate. Temperature gradients are large. Liebermann and Wang (1992) have determined that gradients of 200 K/mm can exist in the hot zone of the furnace in configurations similar to ours. Even if the sample itself is not deforming in a large temperature gradient, the temperature indicated by the thermocouple without careful calibration can be far from the actual sample temperature. We estimate our absolute determinations of run temperature may be in error by as much as 75 K at the present time. However, our calibrations of central temperature vs. furnace power (Fig. 5) indicate reproducibility of T for similar cells under similar conditions to be well under 50 K (i.e., within 25 K of a mean value). Uncertainty between steps in the same experiment must be considerable better; we take them to be ±10 K. Estimating uncertainty in differential stress is an ongoing exercise. Measurement reproducibility, which we estimate from the scatter of points for a given ($h\,k\,l$) Bragg reflection, is approximately ±0.05 GPa in Fig. 6. In this figure, there are obvious examples of points well outside this range;

Table 1
Summary of measurements

Run	$\dot{\varepsilon}$	(±): 4%	T (K)	T (±)[a]	P (GPa)	±
140	1.5×10^{-5}	5.8×10^{-7}	1540	25	4.2	0.05
144(1)	1.9×10^{-5}	7.6×10^{-7}	1477	10	2.7	0.05
144(2)	1.6×10^{-5}	5.2×10^{-7}	1465	10	4.8	0.05
145(1)	1.9×10^{-6}	7.5×10^{-8}	1453	25	4.9	0.05
145(2)	3.2×10^{-5}	1.3×10^{-6}	1451	25	4.9	0.05

Run	σ bulk	σ (1 3 1)	σ (1 1 2)	σ (1 2 2)
140	0.25	0.29	0.25	0.28
144(1)	0.30	0.26	0.28	0.39
144(2)	0.50	0.53	0.47	0.52
145(1)	0.25	0.058	0.053	0.19
145(2)	0.54	0.52	0.39	0.46

[a] Uncertainty relative to run 144, measurement uncertainty approximately 0.05 GPa.

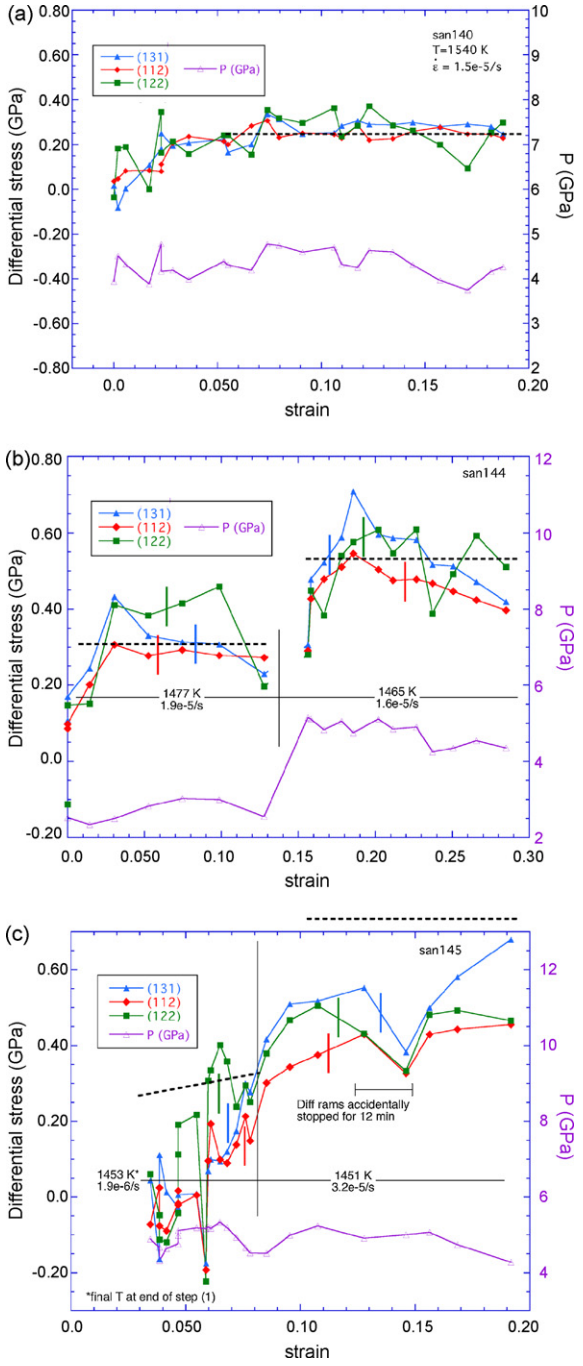

Fig. 6. Stress–strain records for all 3 runs in the hybrid cell: (a) run san140, which was a single-step experiment; (b) run san144, two deformation steps; (c) run san145, two deformation steps. Shown are creep curves measured at three prominent ($h\,k\,l$) Bragg reflections in olivine. Dashed line is the best fit using parameters $\log A = 4.08$, $n = 3.5$, $E^* = 500{,}000$ J/mol, $V^* = 9.5 \times 10^{-6}$ m/mol. Short vertical lines associated on each curve illustrate the 0.05 GPa enclose most of the measurement scatter. Temperature decreased steadily during the first step of run san145 in (c) from 1473 to 1453 K causing the dashed line fit to tilt. An inadvertent 12-min halt of the deformation rams in the middle of the second step in (c) caused a relaxation of differential stress.

these remain unexplained. Pressure, calculated from the equation of state using standard powder diffraction determination of unit cell volume, is accurate to roughly 0.05 GPa.

The nature of the measurement of stress based on X-ray diffraction is such that during deformation one often observes a different state of stress at every diffraction condition. In Fig. 6(a)–(c) for

Please cite this article in press as: Durham, W.B., et al., New measurements of activation volume in olivine under anhydrous conditions. Phys. Earth Planet. Interiors (2008), doi:10.1016/j.pepi.2008.07.045

example, the three most prominent diffraction peaks ($h\,k\,l$) = (1 3 1), (1 1 2), and (1 2 2) produce three different creep curves, with (1 1 2) tending to show a slightly lower differential stress than the others. The cause of the variation with ($h\,k\,l$) reflection is now widely appreciated to be plastic anisotropy of crystals, that is, different slip systems having different flow stresses (see, for example, Weidner et al., 2004; Merkel, 2006). Almost immediately following first plastic yield, the anisotropy of slip can cause the material's elastic state to vary from grain to grain in a way that is not randomly oriented with respect to relevant external reference frames, namely, the applied deviatoric stress field and the geometry of the X-ray beam and detection hardware.

What is not yet so easily understood is how to convert several creep curves into terms such as Eq. (2) that allow convenient application to dynamical processes in the Earth. As stress resolution improves with new hardware and new techniques as it promises to do, the separate flow laws may be probed for their individual implications, and integrated in some way for their broader meaning. It is a matter of much current attention.

The data in Table 1 allow us to constrain the flow parameters A and V^* in Eq. (2). The one attempt to determine the stress exponent n, namely run san145, produced an apparent work hardening during the first step, which ran for 12 h at a slower strain rate. Some of the rise in differential stress was caused by a 20-K downward drift in temperature during the course of deformation at constant displacement rate. The temperature for san145 was calibrated after the run, wherein we discovered that rather than requiring a fixed level of power given by Fig. 5, constant temperature requires upward adjustments of power over time. The effect of holding power constant is small for most run steps, but is not negligible for a 12-h step. The slope of the dashed line in Fig. 6(c) illustrates the temperature effect: only part of the stress increase with strain is thus accounted for. More experimentation is required to determine if the balance is somehow related to the long duration of the step (approximately four times longer than any other step) or is anomalous.

Using values from the literature of $n = 4$ and $E^* = 500$ kJ/mol (Hirth and Kohlstedt, 2003), the differential measurement of run san144 yields $V^* = 9.5 \times 10^{-6}$ m^3/mol. Fig. 7 illustrates this fit with respect to the other measurements as well as the uncertainty range of $\pm 7 \times 10^{-6}$ m^3/mol defined by the error bars. The parameter A, which sets the level of the dashed line fits in the coordinates of Fig. 6(a)–(c), was chosen to be consistent with the strengths seen in san140 and san144; as a result, it is nearly inconsistent (but still within uncertainty limits, see below) with the strength of san145.

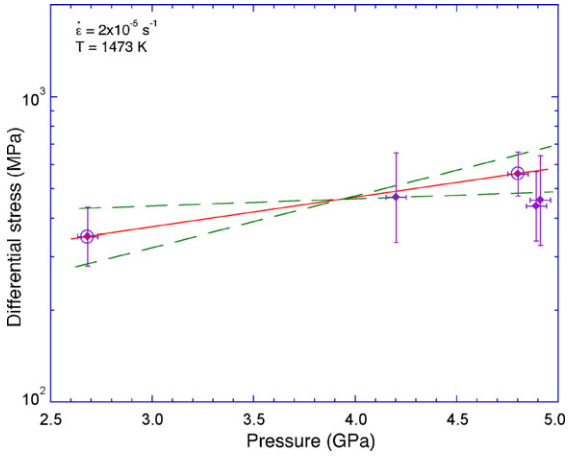

Fig. 7. The five measurements from the hybrid cell reduced to a common T and as indicated using $n = 3.5$ and $E^* = 500{,}000$ J/mol (Hirth and Kohlstedt, 2003) in Eq. (2). The value of $V^* = 9.5 \times 10^{-6}$ m^3/mol (solid line) is defined by the two points from run 144 (circled). Error bars for those two points allow values from 2.5 to 17×10^{-6} m^3/mol (dashed lines). For purposes of plotting, uncertainty in temperature has been converted to an additional uncertainty in stress using the same values of n and E^* (see text).

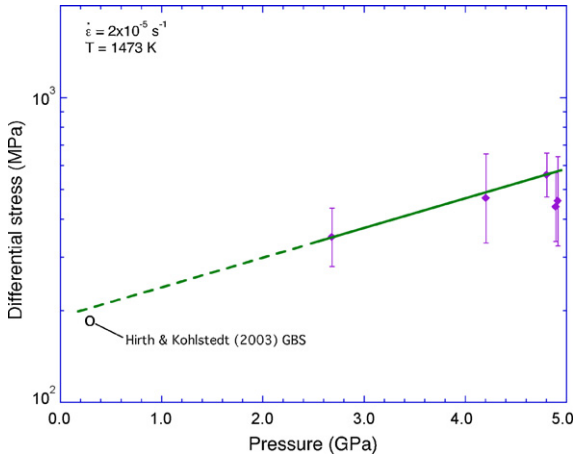

Fig. 8. Comparison of high-pressure D-DIA measurements of "dry" olivine strength to those measured at $P \leq 0.5$ GPa in the gas apparatus. Solid points with error bars and solid line are taken from Fig. 7. Open circle is benchmark for olivine strength at 0.3 GPa under dislocation creep accommodated grain boundary sliding (Hirth and Kohlstedt, 2003).

4. Discussion

4.1. Benchmarking: the strength of olivine

It is critical for validation of the deformation instrument itself, and interesting scientifically, that the measurements in the D-DIA be benchmarked to those of higher resolution, lower pressure instruments. In Fig. 8 we plot our D-DIA measurements with measurements on dry olivine made using a gas apparatus at $P \leq 0.5$ GPa. The benchmarking in Fig. 8 is directed at the pre-exponential constant A in Eq. (2) because as explained above, the measurements here with the D-DIA are too few to allow independent determination of stress exponent n and activation energy E^*. Based on the flow laws given by Hirth and Kohlstedt (2003), we may expect the deformation mechanism under current conditions (dry, grain size approximately 10 μm, $T \leq 1500$ K) to be in the grain-boundary sliding (GBS) regime with necessary grain shape accommodation provided by dislocation slip. The precise match of our current measurements to the established strength of olivine at 0.3 GPa (Fig. 8) is surely fortuitous given the magnitude of our measurement uncertainty, but the consistency of ours with established data is clear. This benchmark is important for the instrument: the flow stress (that is, strength at a given strain rate) of olivine observed with the D-DIA is approximately the same as would be observed in the gas apparatus at identical conditions. We have then, encouraging validation of the accuracy of stress measured at high pressure. Better resolution of the flow law parameters with the D-DIA awaits better precision of stress.

4.2. Comparison to other measurements in the D-DIA

There have been other recent attempts to measure activation volume of olivine using synchrotron X-rays and the D-DIA or similar instruments, including our own work using predecessors to the anhydrous, thermocouple-free cell used here for the first time (Mei et al., manuscript in preparation). The experiments of Li et al. (2004) determined a very low value for V^* of $<5 \times 10^{-6}$ m^3/mol

Please cite this article in press as: Durham, W.B., et al., New measurements of activation volume in olivine under anhydrous conditions. Phys. Earth Planet. Interiors (2008), doi:10.1016/j.pepi.2008.07.045

using stress relaxation experiments in a hydrostatic DIA. Because those measurements were made at high stresses and low plastic strains, the results may not be directly comparable to the measurements reported here. In experiments under stresses and to plastic strains similar to those in our experiments, and using the same D-DIA, Li et al. (2006) again measured a value of V^* near 0. We cannot reconcile our data with theirs, although we can point out a difference in water content. Their experiments were conducted using a pressure medium of amorphous boron powder in epoxy, in contrast with the mullite-based hybrid cell used in our runs. Their samples had a significantly higher water content (~3500 ppm) than ours (≤40 ppm). On the other hand, the results of Borch and Green (1989) suggest that water enhances the pressure sensitivity of creep, at least to $P = 2$ GPa.

Raterron et al. (this volume) have recently found that two important slip systems in olivine have contrasting values for V^*. For a-slip, that is, (0 1 0)[1 0 0], $V^* = 12 \pm 4 \times 10^{-6}$ m^3/mol; while for c-slip, that is (0 1 0)[0 0 1], $V^* = 3 \pm 4 \times 10^{-6}$ m^3/mol. These authors observe that a-slip dominates below $P \approx 8$ GPa at high temperature. In our experiments, a-slip was probably quite active, and thus our value of $V^* = 9.5 \pm 7 \times 10^{-6}$ m^3/mol should be compared to that of $V^* = 12 \pm 4 \times 10^{-6}$ m^3/mol from the Raterron et al. (this volume) study. Thus, the possibility that creep in the polycrystal is controlled by a-slip cannot be eliminated.

Acknowledgments

We gratefully acknowledge the support of the Office of Basic Energy Sciences of the Department of Energy's Office of Science through grant DE-FG02-07ER15839. These experiments would not have been possible without the enthusiastic contribution of Kurt Leinenweber, who perceived the means for making the unusual parts for the hybrid cells, and produced them for us in quantity in a very short time, and we thank the COsortion for Materials Properties Research in Earth Sciences (COMPRES) for supporting Leinenweber's work.

References

Bejina, F., Jaoul, O., Liebermann, R.C., 1999. Activation volume of Si diffusion in San Carlos olivine: implications for upper mantle rheology. Journal of Geophysical Research-Solid Earth 104 (B11), 25529–25542.
Bejina, F., Raterron, P., Zhang, J., Jaoul, O., Liebermann, R.C., 1997. Activation volume of silicon diffusion in San Carlos olivine. Geophysical Research Letters 24 (21), 2597–2600.
Borch, R.S., Green, H.W., 1987. Dependence of creep in olivine on homologous temperature and its implications for flow in the mantle. Nature 330 (6146), 345–348.
Borch, R.S., Green II., H.W., 1989. Deformation of peridotite at high pressure in a new molten cell: comparison of traditional and homologous temperature treatments. Physics of the Earth and Planetary Interiors 55, 269–276.
Dohmen, R., Chakraborty, S., Becker, H.W., 2002. Si and O diffusion in olivine and implications for characterizing plastic flow in the mantle. Geophysical Research Letters 29 (21).
Durham, W.B., Rubie, D.C., 1998. Can the multianvil apparatus really be used for high-pressure deformation experiments? In: Manghnani, M., Yagi, Y. (Eds.), Properties of Earth and Planetary Materials at High Pressure and Temperature, Geophysical Monograph 101. American Geophysical Union, Washington, DC, pp. 63–70.
Durham, W.B., Weidner, D.J., Karato, S.I., Wang, Y.B., 2002. New developments in deformation experiments at high pressure. In: Karato, S.-i., Wenk, H.R. (Eds.), Plastic Deformation of Minerals and Rocks (Reviews in Mineralogy and Geochemistry vol 51). Reviews in Mineralogy & Geochemistry. Mineralogical Society of America, Washington, DC, pp. 21–49.
Griggs, D.T., Turner, F.J., Heard, H.C., 1960. Deformation of rocks at 500° to 800 °C. In: Griggs, D.T., Handin, J.W. (Eds.), Rock Deformation, Geol. Soc. Am. Memoir, vol. 79. Geol. Soc. Am., New York, pp. 39–104.
Hirth, G., Kohlstedt, D.L., 1996. Water in the oceanic upper mantle; implications for rheology, melt extraction and the evolution of the lithosphere. Earth and Planetary Science Letters 144, 93–108.
Hirth, G., Kohlstedt, D.L., 2003. Rheology of the upper mantle and the mantle wedge: a view from the experimentalists. In: Eiler, J. (Ed.), Inside the Subduction Factory. American Geophysical Union, Washington, DC, pp. 83–105.
Jaoul, O., 1990. Multicomponent diffusion and creep in olivine. Journal of Geophysical Research-Solid Earth and Planets 95 (B11), 17631–17642.
Karato, S., Rubie, D.C., Yan, H., 1993. Dislocation recovery in olivine under deep upper-mantle conditions—implications for creep and diffusion. Journal of Geophysical Research-Solid Earth 98 (B6), 9761–9768.
Karato, S.I., Jung, H., 2003. Effects of pressure on high-temperature dislocation creep in olivine. Philosophical Magazine 83 (3), 401–414.
Kohlstedt, D.L., Mackwell, S.J., 1998. Diffusion of hydrogen and intrinsic point defects in olivine. Zeitschrift fur Physikalische Chemie 207, 147–162.
Kohlstedt, D.L., Nichols, H.P.K., Hornack, P., 1980. The effect of pressure on the rate of dislocation recovery in olivine. Journal of Geophysical Research 88, 3122–3130.
Li, L., Weidner, D., Raterron, P., Chen, J.H., Vaughan, M., 2004. Stress measurements of deforming olivine at high pressure. Physics of the Earth and Planetary Interiors 143–144, 357–367.
Li, L., et al., 2006. Deformation of olivine at mantle pressure using the D-DIA. European Journal of Mineralogy 18 (1), 7–19.
Liebermann, R.C., Wang, Y., 1992. Characterization of sample environment in a uniaxial split-sphere apparatus. In: Syono, Y., Manghnani, M.H. (Eds.), High-Pressure Research: Application to Earth and Planetary Sciences. Am. Geophys. Un., Washington, DC, pp. 19–31.
Merkel, S., 2006. X-ray diffraction evaluation of stress in high pressure deformation experiments. Journal of Physics-Condensed Matter 18 (25), S949–S962.
Paterson, M.S., 1982. The determination of hydroxyl by infrared-absorption in quartz, silicate-glasses and similar materials. Bulletin De Mineralogie 105 (1), 20–29.
Poirier, J.-P., 1985. Creep of Crystals. Cambridge University Press, New York, 260 pp.
Poirier, J.-P., Liebermann, R.C., 1984. On the activation volume for creep and its variation with depth in the Earth's lower mantle. Physics of the Earth and Planetary Interiors 35, 283–293.
Raterron, P., Amiguet, E., Chen, J., Li, L. and Cordier, P., this volume. Experimental deformation of olivine single crystals at mantle pressures and temperatures.
Ross, J.V., Avé Lallemant, H.G., Carter, N.L., 1979. Activation volume for creep in the upper mantle. Science 203, 261–263.
Singh, A.K., 1993. The lattice strain in a specimen (cubic system) compressed nonhydrostatically in an opposed anvil device. Journal of Applied Physics 73, 4278–4286.
Singh, A.K., Balasingh, C., Mao, H.-k., Hemley, R., Shu, J., 1998. Analysis of lattice strains measured under nonhydrostatic pressure. Journal of Applied Physics 83 (12), 7567–7578.
Wang, Y., Durham, W.B., Getting, I.C., Weidner, D.J., 2003. The deformation-DIA: a new apparatus for high-temperature triaxial deformation to pressures up to 15 GPa. Review of Scientific Instruments 74, 3002–3011.
Wang, Z., 2002. Effects of Pressure and Water on the Kinetic Properties of Olivine. University of Minnesota 134.
Weidner, D.J., Li, L., Davis, M., Chen, J., 2004. Effect of plasticity on elastic modulus measurements. Geophysical Research Letters 31, doi:10.1029/2003GL019090.
Yamazaki, D., Karato, S., 2001. High pressure rotational deformation apparatus to 15 GPa. Review of Scientific Instruments 72, 4207–4211.

Please cite this article in press as: Durham, W.B., et al., New measurements of activation volume in olivine under anhydrous conditions. Phys. Earth Planet. Interiors (2008), doi:10.1016/j.pepi.2008.07.045